Exchange and crystal field in Sm-based magnets. II. Phenomenological analysis and density functional calculations

Michael D. Kuz'min, Lutz Steinbeck, and Manuel Richter
Institut für Festkörper- und Werkstofforschung, Postfach 270016, 01171 Dresden, Germany
(Received 28 August 2001; published 14 January 2002)

A technique of determining the exchange field B_{ex} on the $4f$ shell of Sm atoms in Sm-based magnets is proposed. It makes use of the $4f$ intermultiplet transition in Sm, observed in inelastic neutron scattering (INS) experiments. The method is used to analyze previously published data for a number of Sm-Fe and Sm-Co intermetallics, for all of which B_{ex} is determined. Additional information on intramultiplet transitions in $SmCo_5$ and Sm_2Co_{17} makes it possible to obtain more accurate B_{ex} values as well as to estimate the leading crystal field parameter (CFP) A_2^0 for these compounds. For the same systems an independent determination of A_2^0 is carried out using published magnetization curves and the B_{ex} values found from the INS spectra. The two "experimental" values of A_2^0 (INS and magnetization) agree well. For comparison, theoretical Sm-Co exchange fields and CFP for $SmCo_5$ and Sm_2Co_{17} are obtained from full-potential density-functional calculations. The theoretical $A_2^0\langle r^2\rangle$ are shifted toward more negative values with respect to their experimental counterparts by a few millielectronvolts. The calculated Sm-Co exchange fields are in fair agreement with the experimentally determined values of the *total* exchange field on Sm, B_{ex}, the weak Sm-Sm exchange interaction being accountable for the remaining small discrepancies.

DOI: 10.1103/PhysRevB.65.064409 PACS number(s): 78.70.Nx

I. INTRODUCTION

The exchange field on the rare earth is a parameter important for the performance of modern permanent magnet materials, many of which are based on Sm-Fe or Sm-Co intermetallics. The importance of B_{ex} derives from the fact that in the temperature range relevant to industrial applications, $T \gtrsim 300$ K, the major part of the anisotropy energy—the single-ion anisotropy due to the rare earth—is proportional to the leading crystal field parameter (CFP) A_2^0 times B_{ex}^2.[1] Experimental determination of B_{ex} has proved difficult because most observable quantities depend simultaneously on B_{ex} and a few unknown CFP. This results in a broad scattering of experimentally found values of B_{ex} and CFP; see, e.g., Table 1 of Ref. 2. This uncertainty, in turn, hampers the development of theoretical methods.

The main objective of this work is therefore to establish a reliable method of determining B_{ex} in such Sm-based materials where the exchange interaction is at least as strong as the crystal field interaction. We turn our attention to the $4f$ intermultiplet transition in Sm, usually visible in inelastic neutron scattering (INS) spectra as a peak at about 0.17 eV. In the following section, it is shown that to know the precise position of this peak is sufficient for a rough estimate of B_{ex}. In this way, values of B_{ex} are obtained for a number of Sm-Fe and Sm-Co intermetallics.

The error bar on these estimates can be nearly halved if the leading CFP A_2^0 is known with rather modest precision. Such information can also be obtained in INS experiments when the so-called intramultiplet transitions are observed at lower energy transfer (even though such experiments are hampered by the neutron absorption resonance at $\sim$0.1 eV in the ^{149}Sm nuclei). Thus Sec. III is dedicated to a joint analysis of inter- and intramultiplet transitions in $SmCo_5$ and Sm_2Co_{17}, leading to more accurate values of B_{ex} and to estimates of A_2^0.

Density-functional calculations of B_{ex} and CFP for $SmCo_5$ and Sm_2Co_{17} are presented in Sec. IV. Section V contains a discussion of the obtained results. Using the B_{ex} values found in Sec. III, A_2^0 for $SmCo_5$ and Sm_2Co_{17} is determined more accurately from published magnetization curves measured on single crystals. These are compared with the A_2^0 values deduced in Sec. III directly from the INS data, as well as with the theoretical values of Sec. IV.

II. ANALYSIS OF THE INTERMULTIPLET TRANSITION ALONE

We start out from the following Hamiltonian, which is defined on the ground *LS* term of samarium (^{6}H) and describes spin-orbit coupling, interaction with an exchange field as well as crystal field effects,

$$\hat{\mathcal{H}} = \lambda \hat{\mathbf{L}} \cdot \hat{\mathbf{S}} + 2\mu_B B_{ex} \hat{S}_z + \hat{\mathcal{H}}_{CF}. \tag{1}$$

A few comments are due in connection with this expression.

(i) The z axis in Eq. (1) has been chosen along the exchange field $\mathbf{B}_{ex}$ which does not necessarily coincide with the crystallographic **c** axis (even though for most hard magnetic materials these two directions do coincide). The CFP's defined in this coordinate system will be denoted as $\mathcal{A}_l^m$, to distinguish them from the "usual" CFP's A_l^m, which enter the crystal field Hamiltonian $\hat{H}_{CF}$ written in the crystallographic coordinates,

$$\hat{H}_{CF} = A_2^0 \sum_i (3z_i^2 - r_i^2) + A_4^0 \sum_i (35z_i^4 - 30z_i^2 r_i^2 + 3r_i^4) + \cdots, \tag{2}$$

where i runs over the electrons of the $4f$ shell of Sm. Note that many of the CFP's A_l^m have been omitted from Eq. (2)

for symmetry reasons. In particular, the uniaxial symmetry of most hard magnetic materials allows just one second-order term, with A_2^0. Many-more low-symmetry terms enter the expression for $\hat{\mathcal{H}}_{\rm CF}$, in which all coefficients $\mathcal{A}_l^m$, $-l \leqslant m \leqslant l$, $l=2,4,6$, are generally nonzero. However, only the terms containing $\mathcal{A}_l^0$ are relevant to our purpose here, which is to compute energy corrections of the first order in $\hat{\mathcal{H}}_{\rm CF}$.

The two sets of CFP's are generally connected by linear transformations, separate for each l. If $\mathbf{B}_{\rm ex} \| \mathbf{c}$, $\mathcal{A}_l^m = A_l^m$.

(ii) The use of *LS* coupling in Eq. (1) is justified by the fact that our analysis will be restricted to the two lowest *J*-multiplets, for which this approximation is known to be valid.[3]

(iii) In the compounds of our interest the strengths of the interactions associated with the three terms in the Hamiltonian, Eq. (1), obey the following hierarchical relation: (spin-orbit)$\gg$(exchange)$\gg$(crystal field).

We begin our approximate analysis of the energy spectrum of this Hamiltonian by neglecting the relatively weak last term in Eq. (1), $\hat{\mathcal{H}}_{\rm CF}$ (its influence will be considered in some detail in Appendix B). The remainder of the Hamiltonian is approximately diagonal in the (JM) representation: the spin-orbit coupling forms the multiplet structure, whereas the main effect of the exchange field is the Zeeman splitting of the multiplets into separate levels, in direct proportion with the magnetic quantum number M. The exchange term also has nondiagonal matrix elements, whose presence leads to mixing of the states with the same M but different J's. Since we regard the exchange interaction as a perturbation with respect to the stronger spin-orbit coupling, in the first approximation the J mixing is neglected and the eigenvalues are

$$E_{JM} = \tfrac{1}{2}\lambda[J(J+1) - L(L+1) - S(S+1)] + 2(g_J - 1)M\mu_B B_{\rm ex} \tag{3}$$

where g_J is the Landé splitting factor. For the lowest two multiplets of samarium, $^6H_{5/2}$ and $^6H_{7/2}$, the Landé factors are $g_{5/2}=2/7$ and $g_{7/2}=52/63$.

According to Ref. 4, the intensity of a dipole transition between the states $|JM\rangle$ and $|J+1,M'\rangle$ is proportional to the square of the following $3j$ symbol:

$$\begin{pmatrix} J+1 & 1 & J \\ -M' & M'-M & M \end{pmatrix}.$$

Numerical values of the squares of the three nonzero $3j$ symbols (with $M-M'=0,\pm 1$) relevant to the ground state of Sm^{3+}, $J=M=5/2$, can be found, e.g., on p. 49 of Ref. 5. Thus one concludes that the intensities of the three allowed intermultiplet transitions from the ground state of Sm $|\frac{5}{2}\frac{5}{2}\rangle$ are related as 1:6:21, the most intensive one being between $|\frac{5}{2}\frac{5}{2}\rangle$ and the lowest level of the first excited multiplet $|\frac{7}{2}\frac{7}{2}\rangle$. As follows from Eq. (3), the corresponding transition energy is

$$E_{\rm inter} = E_{7/2\,7/2} - E_{5/2\,5/2} = \Delta_{\rm so} + \tfrac{148}{63}\mu_B B_{\rm ex}, \tag{4}$$

TABLE I. Observed intermultiplet transition energies $E_{\rm inter}$ and the exchange fields on Sm, $B_{\rm ex}$, obtained from $E_{\rm inter}$ by means of Eq. (5). The values of $B_{\rm ex}$ are accurate to ± 40 T.

Compound	$E_{\rm inter}$ (meV)	$B_{\rm ex}$ (T)
$SmCo_5$	165.7[a]	310
Sm_2Co_{17}	161[b]	270
Sm_2Fe_{17}	176 ± 2[c]	380
$Sm_2Fe_{17}N_3$	163[d]	290
$Sm_2Fe_{14}B$	179 ± 2[e]	400
$SmFe_{11}Ti$	175.5[f]	380

[a]Ref. 2
[b]Ref. 7.
[c]Average of Refs. 8 and 9.
[d]Ref. 9.
[e]Ref. 10.
[f]Ref. 11.

where $\Delta_{\rm so}=\frac{7}{2}\lambda$ is the spin-orbit splitting between the ground and first excited multiplets. For samarium, $\Delta_{\rm so}=124$ meV (Table 5.3 of Ref. 6).

In a compound where Sm atoms are subject to a strong exchange field, observation of the intermultiplet transition at $E_{\rm inter}$ provides a ready estimate of that exchange field:

$$\mu_B B_{\rm ex} = \tfrac{63}{148}(E_{\rm inter} - \Delta_{\rm so}). \tag{5}$$

This simple formula neglects J mixing and crystal field effects. Analysis presented in Appendix A shows that J mixing is in principle unable to shift $E_{\rm inter}$ in Sm by more than 0.3 meV. This is far less than the accuracy of experimental determination of $E_{\rm inter}$ (± 2 meV). Therefore, when treating INS data on the intermultiplet transition in samarium, J mixing can be safely neglected.

Regarding the crystal field effects, the situation is slightly more complicated. The only sizable corrections come from the diagonal in the (JM) representation matrix elements of $\hat{\mathcal{H}}_{\rm CF}$, the most important of them being proportional to $\mathcal{A}_2^0$. (Note our use of CFP's defined in the coordinate system with $\mathbf{z} \| \mathbf{B}_{\rm ex}$.) The joint contribution to $E_{\rm inter}$ from the higher-order terms $\mathcal{A}_4^0$ and $\mathcal{A}_6^0$ does not exceed 1 meV (see Appendix B for proof) and will be neglected. When the contribution from $\mathcal{A}_2^0$ is taken into consideration (Appendix B), Eq. (5) becomes

$$\mu_B B_{\rm ex} = \tfrac{63}{148}(E_{\rm inter} - \Delta_{\rm so}) + \tfrac{26}{925}\mathcal{A}_2^0\langle r^2\rangle. \tag{6}$$

If no information on the value of $\mathcal{A}_2^0$ is available, one can simply put $\mathcal{A}_2^0\langle r^2\rangle = \pm 30$ meV in Eq. (6), which converts it into Eq. (5) with an extra uncertainty of ± 2 meV added to $E_{\rm inter}$ (30 meV is the strongest crystal field encountered in intermetallic compounds). The overall uncertainty in $B_{\rm ex}$ is then ± 40 T. The advantage of Eq. (5) is that one need not take any care of the actual orientation of the easy magnetization direction in the crystal.

Thus Table I contains values of the exchange field on samarium, $B_{\rm ex}$, obtained from the intermultiplet transition

energies E_{inter} (Refs. 2, 7, 8, 10 and 11) for some Sm-Co and Sm-Fe intermetallics using Eq. (5) with $\Delta_{\text{so}}=124$ meV.

III. COMBINED ANALYSIS OF THE INTER- AND INTRAMULTIPLET TRANSITIONS

In some Sm-Co intermetallics, along with the intermultiplet transition at high energies, an intramultiplet transition has been observed in the low-energy range $E_{\text{intra}}\sim 20-30$ meV. The purpose of this section is to demonstrate that knowledge of both E_{inter} and E_{intra} leads to a more accurate determination of B_{ex} than the one afforded by Eq. (5) on the basis of E_{inter} alone, as well as yielding an estimate of the leading crystal field parameter $\mathcal{A}_2^0$.

We begin by writing out approximate eigenvalues E_{JM} of the Hamiltonian (1) within the ground ($J=5/2$) multiplet of samarium:

$$B_{(5/2)M}=-15\lambda-\frac{10}{7}M\mu_B B_{\text{ex}}+\frac{30}{49}\left(M^2-\frac{49}{4}\right)\frac{(\mu_B B_{\text{ex}})^2}{\Delta_{\text{so}}}+\frac{13}{315}\mathcal{A}_2^0\langle r^2\rangle\left[3M^2-\frac{35}{4}\right]+\frac{26}{10\,395}\mathcal{A}_4^0\langle r^4\rangle\left[35M^4-\frac{475}{2}M^2+\frac{2835}{16}\right]. \quad (7)$$

Here the first two terms are just the diagonal matrix elements of the spin-orbit and exchange terms of Eq. (1), or Eq. (3) with 5/2 substituted for J. The last two terms in Eq. (7) come from the diagonal in the (JM) representation matrix element of the crystal field Hamiltonian, $\langle \frac{5}{2}M|\hat{\mathcal{H}}_{\text{CF}}|\frac{5}{2}M\rangle$. Within the ground multiplet the standard Stevens formalism applies: thus the prefactors of the crystal field terms in Eq. (7) are the usual Stevens coefficients and the somewhat unfamiliar-looking expressions in square brackets are in fact the well-known Stevens operators O_2^0 and O_4^0, with 5/2 and M substituted for J and J_z, respectively. Note that there is no sixth-order contribution since $\gamma_{5/2}=0$.

The third term in Eq. (7) describes the effect of J mixing. It is an energy correction of second order in the exchange operator $2\mu_B B_{\text{ex}}\hat{S}_z$, which is regarded as a perturbation with respect to the spin-orbit coupling. The operator $\hat{S}_z$ connects states with equal quantum numbers M for which $\Delta J=\pm 1$; therefore, $|\frac{5}{2}M\rangle$ only interacts with $|\frac{7}{2}M\rangle$. The following expression, a particular case of Van Vleck's formula,[12] was used: $\langle \frac{7}{2}M|\hat{S}_z|\frac{5}{2}M\rangle^2=\frac{15}{98}\,[(\frac{7}{2})^2-M^2]$, where the prefactor $\frac{15}{98}$ is just the square of the quantity $\langle J+1\|\Lambda\|J\rangle$ taken from Table 2 of Ref. 13.

The most intensive intramultiplet transition is from the ground state $|\frac{5}{2}\frac{5}{2}\rangle$ to the first excited level $|\frac{5}{2}\frac{3}{2}\rangle$. As follows from Eq. (7), the energy of this transition is given by

$$E_{\text{intra}}=E_{5/2\,3/2}-E_{5/2\,5/2}=\frac{10}{7}\mu_B B_{\text{ex}}-\frac{120}{49}\frac{(\mu_B B_{\text{ex}})^2}{\Delta_{\text{so}}}-\frac{52}{105}\mathcal{A}_2^0\langle r^2\rangle-\frac{416}{693}\mathcal{A}_4^0\langle r^4\rangle. \quad (8)$$

TABLE II. Exchange field B_{ex} and crystal field parameter $A_2^0\langle r^2\rangle$ for Sm in $SmCo_5$ and Sm_2Co_{17} obtained from inelastic neutron scattering (INS) and magnetization data and from density functional (DF) calculations.

	$SmCo_5$	Sm_2Co_{17}	Comment
B_{ex} (T)	295 (25)	266 (25)	from INS[a]
	291	298	DF calculation, Sm-Sm exchange neglected
$A_2^0\langle r^2\rangle$ (meV)	−24 (7)	−12 (7)	From INS[b]
	−22 (3)	−10 (1)	From magnetization[c]
	−31	−16	DF calculation

[a]Equation (10) with data from Ref. 9.
[b]Equation (9) with data from Ref. 9.
[c]From fitting the data of Refs. 29 and 31.

This formula is correct to first order in the crystal field and to third order in B_{ex} (it can be shown that in samarium E_{intra} contains no term $\propto[\mu_B B_{\text{ex}}]^3/\Delta_{\text{so}}^2$ because the corresponding third-order corrections to $E_{5/2\,5/2}$ and $E_{5/2\,3/2}$ are fortuitously equal).

The last term in Eq. (8) is the least important. If no information is available on the value of $\mathcal{A}_4^0$ in the system under study (which is often the case), one can assume broadly that $\mathcal{A}_4^0\langle r^4\rangle=\pm 3$ meV. The last term can then be omitted from Eq. (8) at the expense of adding an extra uncertainty of ± 2 meV to the experimentally determined E_{intra}. The gain, however, is that without the last term, Eq. (8) can be readily rewritten so as to make it suitable for evaluating $\mathcal{A}_2^0$:

$$\mathcal{A}_2^0\langle r^2\rangle=-\frac{105}{52}E_{\text{intra}}+\frac{75}{26}\mu_B B_{\text{ex}}-\frac{450}{91}\frac{(\mu_B B_{\text{ex}})^2}{\Delta_{\text{so}}}. \quad (9)$$

Thus, if in addition to an intermultiplet transition at E_{inter} an intramultiplet transition is observed at E_{intra} in an exchange-dominated samarium compound, one can substitute Eq. (9) into Eq. (6) and solve the resulting quadratic equation for $\mu_B B_{\text{ex}}$:

$$\mu_B B_{\text{ex}}=\left[\left(\tfrac{119}{36}\,\Delta_{\text{so}}\right)^2+\tfrac{49}{16}\,\Delta_{\text{so}}(E_{\text{inter}}-\Delta_{\text{so}})-\tfrac{49}{120}\,\Delta_{\text{so}}E_{\text{intra}}\right]^{1/2}-\tfrac{119}{36}\,\Delta_{\text{so}}. \quad (10)$$

The use of Eq. (10), followed by Eq. (9), produces an immediate numerical result for the pair of parameters $(B_{\text{ex}},\mathcal{A}_2^0)$. Table II contains the results obtained in this way for $SmCo_5$ ($E_{\text{intra}}=30.7$ meV) (Ref. 2) and Sm_2Co_{17} ($E_{\text{intra}}=23.3$ meV) (Ref. 7).

The accuracy of these results is more readily estimated by considering Eqs. (6) and (9) separately. Much of the uncertainty in B_{ex} values obtained from Eq. (5) was due to the lack of knowledge of $\mathcal{A}_2^0\langle r^2\rangle$, replaced in Eq. (6) by ± 30 meV. Assuming that $\mathcal{A}_2^0$ is now known reduces the uncertainty in B_{ex} from ± 40 to ± 25 T. The error in $\mathcal{A}_2^0\langle r^2\rangle$ is $\pm$ [6 meV $+2\times(\text{error in}E_{\text{intra}})]\approx\pm 7$ meV. Both $SmCo_5$ and Sm_2Co_{17} are easy-axis magnets, so one need not distinguish between $\mathcal{A}_2^0$ and A_2^0.

The method used to obtain the density-functional results included in Table II is described in the following section, and the fitting of magnetization data is described in Sec. V.

IV. DENSITY-FUNCTIONAL CALCULATION OF SM-CO EXCHANGE FIELD AND CRYSTAL FIELD PARAMETERS

The new, more reliable estimates of B_{ex} and A_2^0 in $SmCo_5$ and Sm_2Co_{17} obtained in the previous section allow a reassessment of the theoretical CFP's obtained from density-functional (DF) calculations. A proper judgment about the quality of the DF results has previously been impeded by the large uncertainty of the experimental values. On the other hand, we have improved our method of calculation with respect to earlier work.[14–16] For that reason, we recalculate the CFP's of $SmCo_5$ and Sm_2Co_{17} with the more refined method in order to compare the new experimental $A_2^0\langle r^2\rangle$ with state-of-the-art theoretical results. Furthermore, we calculate the Sm-Co exchange field from the change in total energy upon rotation of the Sm $4f$ spins, as described in Ref. 17. In the following, we briefly outline our method, with particular emphasis on the improvements with respect to our earlier work.

Equating the nonspherical part of the Hartree and (linearized) exchange-correlation interaction energy[16] of the $4f$ electrons with all other charges in the crystal with the expectation value of the CF Hamiltonian yields the following formula for the CFP:

$$A_l^m\langle r^l\rangle = C_{lm}\int dr\, r^2 R_{4f}^2(r) V_{lm}(r). \tag{11}$$

The components $V_{lm}(r)$ of an expansion of the crystal potential into real spherical harmonics centered at the rare-earth site are obtained from a self-consistent DF calculation within the local spin density approximation (LSDA). In this calculation, the $4f$ states are treated as open core states where the ground-state configuration and Russell-Saunders spin moment are fixed. The $4f$ charge density is spherically averaged in order to eliminate self-interaction contributions to the CF from the nonspherical $4f$ charge density. The other quantities entering Eq. (11) are the radial expectation value

$$\langle r^l\rangle = \int dr\, r^{l+2} R_{4f}^2(r), \tag{12}$$

the prefactors C_{lm} as defined by Hutchings,[18] and the $4f$ radial charge density $R_{4f}^2(r)$, normalized to yield $\langle r^0\rangle = 1$. The two ingredients needed to calculate the CFP's, Eq. (11), are (i) the nonspherical components $V_{lm}(r)$ of the potential in the region of non vanishing $4f$ density around the considered rare-earth site and (ii) the $4f$ radial wave function $R_{4f}(r)$. The nonspherical crystal potential is naturally obtained from a full-potential calculation. Because of the overlap between the $4f$ charge density and the charges creating the CF, the CFP's are sensitive to the shape of the radial $4f$ density, in particular to its behavior at larger distance from the nucleus. The latter behavior is poorly described by the standard LSDA yielding $4f$ states which are severely underbound and hence much too delocalized as a consequence of self-interaction. This can be remedied to a large extent by the self-interaction correction (SIC).[19] Therefore, we treat the $4f$ states in the SIC-LSDA.[16,20]

The present calculations were performed with the scalar-relativistic full-potential local orbital (FPLO) scheme.[21] The Sm $5s$, $5p$, $6s$, $6p$, $5d$ and Co $4s$, $4p$, $3d$ states were treated as valence states. We employed the Perdew-Zunger parametrization[19] of the Ceperley-Alder[22] exchange-correlation potential. The reciprocal-space integrations were done with 133 (13) **k** points in the irreducible part of the hexagonal (rhombohedral) Brillouin zone for the $CaCu_5$ (Th_2Zn_{17}) structure compounds. The experimental lattice parameters $a = 5.004$ Å and $c = 3.969$ Å of $SmCo_5$ (Ref. 23) were used. Since we are not aware of any refined structure data on Sm_2Co_{17}, we took those of Nd_2Co_{17}, $a = 8.398$ Å, $c = 12.218$ Å.[24]

The present work improves on our previous calculations of CFP's for $SmCo_5$ (Ref. 15) and Sm_2Co_{17} (Ref. 16) in various ways: (A) The intra-atomic nonsphericity of the crystal potential is treated in a self-consistent way by employing a proper full-potential method, whereas previously only the nonspherical effects in the interstitial region were treated self-consistently while the full charge density was calculated without shape restrictions only in the final step of the self-consistent cycle. (B) The Sm $5p$ semicore states are included in the valence basis (besides the Sm valence states) in the present calculation since they have been found to contribute significantly to the lowest-order CFP $A_2^0\langle r^2\rangle$. [25] (C) The contribution of the exchange-correlation potential to the CF was taken into account, in contrast to our previously published calculations on $SmCo_5$.

In Table III we compare the CFP of $SmCo_5$ from the present calculation with our previous linear combination of atomic orbitals (LCAO) results[15] and two recent full-potential calculations.[26,27] In order to investigate the influence of (A), (B), and (C), we performed test calculations where (a) the Sm $5p$ states were put into the core and (b) the exchange-correlation contribution to the CF was neglected in addition. As can be seen, the asphericity of the Sm $5p$ shell due to hybridization reduces the second-order CFP by 30%. Neglecting the exchange-correlation contribution changes all the parameters, particularly $A_2^0\langle r^2\rangle$ and $A_4^0\langle r^4\rangle$. The results of test (b) are close to our previous results. This proves that the influence of the self-consistent treatment of the intra-atomic asphericity [(A) above] on the CF is small. Our results agree well with a recent full-potential calculation performed with the full-potential linearized augmented plane wave (FLAPW) method,[26] considering the slightly different treatment of the $4f$ radial wave function in the two calculations. In Ref. 26 the $4f$ radial wave function was taken from a SIC-LSDA calculation for a free Sm^{3+} ion in which the electron occupation numbers were fixed to the values that occur in $SmCo_5$, while in the present work it was calculated self-consistently in the crystal within SIC-LSDA (open core approximation). This has some influence on the higher-order CFP's which are sensitive to the tail of the $4f$ radial wave function. Our results are also in agreement with recent full-

TABLE III. Comparison of the crystal field parameters $A_l^m\langle r^l\rangle$ (in meV) obtained from the present calculation (FPLO, fifth column) for Sm in $SmCo_5$ with previous results obtained with the LCAO method (where the Sm $5p$ valence and exchange-correlation contributions to the CF were not taken into account) in Ref. 15 (second column), the FLAPW method in Ref. 26 (sixth column), and the FLMTO method in Ref. 27 (last column). For comparison, two test results obtained in the present work are also included, where (a) the Sm $5p$ states were treated as core states and (b) the Sm $5p$ states were treated as core states and the contribution of the exchange-correlation potential to the crystal field was neglected.

	LCAO	FPLO test (b)	FPLO test (a)	FPLO	FLAPW	FLMTO
$A_2^0\langle r^2\rangle$	−65.5	−64.3	−44.0	−30.8	−30.1	−30.9
$A_4^0\langle r^4\rangle$	−3.2	−3.9	−2.5	−2.5	−3.2	−1.7
$A_6^0\langle r^6\rangle$	0.9	1.1	1.3	1.3	0.6	
$A_6^6\langle r^6\rangle$	25.0	37.1	46.6	46.2	27.2	

potential linearized muffin-tin orbital (FLMTO) results[27] for the second-and fourth-order CFP's.

A consistent calculation of the total exchange field B_{ex} acting on the $4f$ shell is a difficult task because it contains a contribution from Sm-Sm exchange. In metallic systems this interaction has a long-range character and involves many remote neighbor atoms. It cannot therefore be reduced to an interaction between two sublattices of rare-earth atoms as was assumed in Ref. 28. Neglecting the Sm-Sm exchange significantly simplifies the problem since now B_{ex} is due exclusively to the intersublattice (Sm-Co) exchange which is much more amenable to computational treatment.

The effective Sm-Co exchange field is calculated from the change in the total energy of the system when all $4f$ moments are rotated out of their ground-state orientation by 180°.[17] According to Eq. (1), such a rotation should increment the total energy by $4S\mu_B B_{ex}$ per Sm atom ($S=5/2$), provided the Sm-Sm exchange is neglected. Two separate self-consistent total energy calculations are performed with the spin of the $4f$ open core shell being fixed to an orientation antiparallel and parallel to the Co spins, respectively. In this way, all relaxation effects are included and the change of any contribution to the total energy upon rotation of the $4f$ spin is attributed to the intersublattice exchange interaction (Table II).

V. DISCUSSION

Now we turn our attention to investigating the compatibility of the second-order CFP's deduced in Sec. III with magnetization data and to a comparison of the experimental CFP's obtained from INS and magnetization data with the DF results.

For that purpose, the exchange fields derived from E_{inter} and E_{intra} in Sec. III are used to determine $A_2^0\langle r^2\rangle$ by fitting magnetization curves measured at 4.2 K on $SmCo_5$ (Refs. 29 and 30) and Sm_2Co_{17} (Ref. 31) single crystals. A reliable determination of this parameter from magnetization data has previously been hampered by the lack of direct quantitative experimental information on the exchange field.

The fitting procedure is described in detail in Ref. 32. Therefore, we restrict ourselves to a brief summary of the main points here. For a given temperature T and a magnetic field **B** directed perpendicular to the easy axis **c**, the equilibrium magnetization orientation is determined by minimizing the free energy of the system. This yields the reduced transverse magnetization $m_\perp=\cos(\widehat{M,B})$. The experimental values[33–35] of the zero-temperature Co sublattice magnetization $M_{Co}(0)$ and anisotropy constant $K_1^{Co}(0)$ (taken from the isostructural Y compounds) and Curie temperatures T_C (Ref. 36) were used: see Table IV. The temperature dependence of the Co sublattice anisotropy and magnetization is described by empirical formulas given in Ref. 32, Eqs. (16). The Sm contribution to the free energy is calculated by diagonalizing the Hamiltonian obtained from adding the Zeeman term $\mu_B\mathbf{B}\cdot(2\hat{\mathbf{S}}+\hat{\mathbf{L}})$ to Eq. (1). The three lowest J-multiplets ($J=5/2,7/2,9/2$) are taken into account. Then the measured magnetization curves are fitted by adjusting either $A_2^0\langle r^2\rangle$ only or $A_2^0\langle r^2\rangle$ and $A_4^0\langle r^4\rangle$. The higher-order CFP's are neglected for reasons pointed out in Ref. 32. For the exchange field B_{ex} we use the values from Table II derived from E_{inter} and E_{intra} by means of Eq. (10).

In Fig. 1, the measured reduced transverse magnetizations of $SmCo_5$ (Ref. 29 and 30) and Sm_2Co_{17} (Ref. 31) are shown together with the fit curves. The hard-axis magnetization curve of $SmCo_5$ is well reproduced with $A_2^0\langle r^2\rangle=-25$ meV, $A_4^0\langle r^4\rangle=0$. The magnetic field available in Ref. 29, $B<15$ T, was only able to induce relatively small ($\theta<13°$) deviations of the magnetization vector from the easy direction in $SmCo_5$ (see Fig. 2, where $m_\perp\equiv\sin\theta<0.22$). Within this range of magnetic fields the fourth-order CFP A_4^0

TABLE IV. Experimental data used for fitting the magnetization curves of $SmCo_5$ and Sm_2Co_{17} in the present work. The Co sublattice magnetization $\mu_0 M_{Co}$ and anisotropy constant K_1^{Co} (at 4.2 K) are taken from the isostructural Y compounds.

	$SmCo_5$	Sm_2Co_{17}
$\mu_0 M_{Co}$ (T)	1.15[a]	1.30[b]
K_1^{Co} (MJ/m^3)	7.4[a]	−0.4[b]
T_C (K)	1000[c]	1193[c]

[a]Reference 33.
[b]Reference 34.
[c]Reference 36.

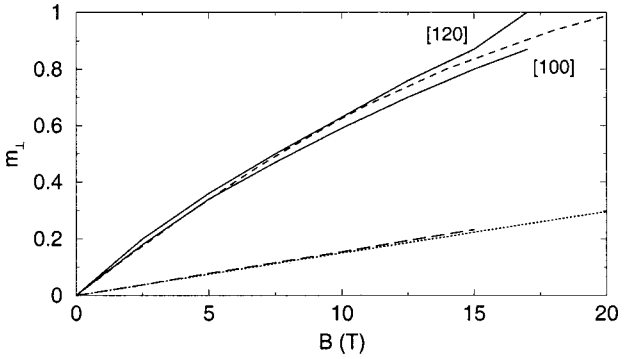

FIG. 1. Transverse reduced magnetization vs magnetic field applied at right angle to the *c* axis at $T=4.2$ K. Sm_2Co_{17}: solid line, experiment (Ref. 31) dashed line, fit, this work. $SmCo_5$: dashed line, experiment (Ref. 29), dotted line, fit, this work.

has little effect on the magnetization curve, since it primarily affects the second anisotropy constant and the corresponding term in the anisotropy energy, $K_2 \sin^4\theta$, is small. Thus taking $A_4^0\langle r^4\rangle = \pm 1$ meV resulted in practically no visible change in the magnetization curve calculated for $SmCo_5$.

Sm_2Co_{17} exhibits a substantial anisotropy within the basal plane. Therefore, two experimental magnetization curves for Sm_2Co_{17} are shown in Fig. 1, measured along the [100] and [120] directions. The fit curve for Sm_2Co_{17} (which was adjusted in such a way as to lie in between the two experimental curves) was obtained with $A_2^0\langle r^2\rangle = -9$ meV and $A_4^0\langle r^4\rangle = -0.3$ meV. Inclusion of a nonzero fourth-order parameter straightens the fit curve somewhat, thus improving agreement with experiment.

The second-order parameters are in satisfactory agreement with the approximate values of -24 and -12 meV estimated by means of Eq. (9) from E_{intra} and E_{inter} of $SmCo_5$ and Sm_2Co_{17}, respectively. The intramultiplet transition energies observed by INS in these two compounds are reproduced within ± 1 meV by the second-order CFP obtained from fitting the magnetization curves. Hence the derived exchange and second-order CFP's simultaneously describe the INS and magnetization data well. Moreover, as B_{ex} is obtained from E_{inter}, which only weakly depends on $A_2^0\langle r^2\rangle$, the $A_2^0\langle r^2\rangle$ values derived from the magnetization curves in this work are much more reliable than previous estimates. The broad scattering of the earlier results (cf. Table I of Ref. 2) arose because it was attempted to obtain both B_{ex} and $A_2^0\langle r^2\rangle$ (and in some cases even higher-order CFP's) from fitting magnetization data alone. The error bar of the exchange fields derived from E_{inter} and E_{intra} is $\pm$ 25 T. This results in an uncertainty of $\pm$ 1 meV in the $A_2^0\langle r^2\rangle$ values obtained from fitting the magnetization data.

Another source of uncertainty in fitting the magnetization data is the Co sublattice anisotropy. It is usually assumed to be equal to that of the isostructural Y compound. DF calculations[37] within the LSDA corrected for orbital polarization revealed, however, a considerable variation of the Co sublattice anisotropy in RCo_5, depending on the rare-earth constituent *R*, as a consequence of changes in the lattice geometry and in the hybridization of the rare-earth valence states. The Co sublattice anisotropy for $SmCo_5$ found from the calculation is $K_1^{\text{Co}}(0) = 13.8$ MJ/m^3, much larger than the value of 7.4 MJ/m^3 measured on YCo_5.[33] The calculations somewhat overestimate the *T* sublattice anisotropy, yielding 9.3 MJ/m^3 for YCo_5. Scaling down the calculated value for $SmCo_5$ by multiplying it with the ratio of measured and calculated $K_1^{\text{Co}}(0)$ of YCo_5 yields $K_1^{\text{Co}}(0) = 10.9$ MJ/m^3. Using this Co sublattice anisotropy constant (instead of that taken from the Y compound) for the fit of the magnetization curve of $SmCo_5$ results in $A_2^0\langle r^2\rangle = -19$ meV. This is in worse agreement with the second-order parameter derived from E_{intra} for this compound.

In the case of Sm_2Co_{17}, the uncertainty resulting from the Co sublattice anisotropy is much smaller. A DF calculation for Sm_2Co_{17} yielded $K_1^{\text{Co}}(0) = -1.7$ MJ/m^3, which is much larger than either calculated or measured for Y_2Co_{17}. Taking this theoretical Co sublattice anisotropy for the fit results in $A_2^0\langle r^2\rangle = -10$ meV, in slightly better agreement with the value deduced from E_{intra}. The appreciable anisotropy within the basal plane introduces an uncertainty in $A_2^0\langle r^2\rangle$ of about ± 0.5 meV, given by the limits of possible fits between the two magnetization curves measured along the [120] and [100] directions.

Table II includes the CFP for Sm in $SmCo_5$ and Sm_2Co_{17} resulting from a DF calculation as outlined in Sec. IV in comparison with the experimental estimates of $A_2^0\langle r^2\rangle$ obtained from analyzing the INS and magnetization data in the present work. We are not aware of any reliable experimental information on the higher-order CFP's for the considered compounds. Both calculated second-order parameters are larger than their experimental counterparts, although the differences between theory and experiment are reduced in comparison with our previous work,[15,16] where the theoretical methods were less refined and the error bars on the experimental values much larger. As already stated in Sec. IV, our present results for $SmCo_5$ are in agreement with other recent full-potential studies.[26,27] Possible reasons for the remaining discrepancy between theory and experiment are (i) the sensitivity of the calculated CFP to the $4f$ radial wave function, which may not be perfectly described even within SIC-LSDA, (ii) the polarization of the inner core states (beside the already mentioned $5p$ of Sm) by the nonspherical crystal potential,[27] which has not been taken into account, and (iii) the influence of spin-orbit coupling on the asphericity of the on-site charge density (particularly, of that associated with the $5d$ and $5p$ states of Sm) and thus on the CF, which has not been investigated so far.

The Sm-Co exchange fields obtained from the DF calculation are also shown in Table II. One can see that they agree well with the experimentally determined values of the *total* exchange field on Sm, B_{ex}. When comparing these two values, one should increment the error bars on B_{ex} by the amount arising from the neglect of the Sm-Sm exchange interaction, $kT_N/\mu_B \approx 13$ T, where $T_N \approx 9$ K is the Néel point of the isomorphous compound $SmCu_5$.[38]

VI. CONCLUSIONS

The exchange field on Sm in compounds with strong exchange interaction can be determined in a simple and reliable

way from INS data on the intermultiplet transition. The method is not restricted to Sm, but equally applies to other rare earths.

Additional information on intramultiplet transitions results in a more accurate determination of B_{ex} and also yields an estimate of the leading CFP A_2^0. The thus obtained values of A_2^0 agree with the ones deduced (using the above B_{ex}) from magnetization curves measured on single crystals.

Density-functional calculations reproduce well the experimental B_{ex} values, with some allowance for the weak Sm-Sm interaction which was neglected in the calculation. The theoretical $A_2^0\langle r^2\rangle$, in both $SmCo_5$ and Sm_2Co_{17}, are found to deviate from the experimental values by roughly -7 meV.

ACKNOWLEDGMENTS

This work was supported by the German Science Foundation, Sonderforschungsbereich 463, Teilprojekte B11, B12. Helpful discussions with P. Novák and V. Nekvasil are gratefully acknowledged.

APPENDIX A: INFLUENCE OF J MIXING ON E_{inter}

Let us consider how the energy of the intermultiplet transition, E_{inter}, is affected by the off-diagonal matrix elements of the operator $2\mu_B B_{ex}\hat{S}_z$ which connect states $|JM\rangle$ with the same M and $\Delta J=\pm 1$. When this operator is regarded as a perturbation with respect to the spin-orbit interaction, the eigenvalues (3) are correct to a first approximation, whereas corrections of second and higher orders describe J mixing.

The bulk of the effect comes from the terms quadratic and cubic in $\mu_B B_{ex}$. In this approximation the energy of the ground state $|\frac{5}{2}\frac{5}{2}\rangle$ is only affected by virtual transitions to and from $|\frac{7}{2}\frac{5}{2}\rangle$ (excitation energy Δ_{so}) and is given by

$$E_{5/25/2}=-15\lambda-\frac{25}{7}\mu_B B_{ex}-\frac{180}{49}\frac{(\mu_B B_{ex})^2}{\Delta_{so}}+\frac{3400}{343}\frac{(\mu_B B_{ex})^3}{\Delta_{so}^2}. \quad \text{(A1)}$$

The first three terms here are readily obtained from Eq. (7) by setting $M=5/2$ and omitting the crystal field terms. The last term is a third-order correction: its prefactor is the following combination of matrix elements:

$$\langle\tfrac{7}{2}\tfrac{5}{2}|2\hat{S}_z|\tfrac{5}{2}\tfrac{5}{2}\rangle^2\{\langle\tfrac{7}{2}\tfrac{5}{2}|2\hat{S}_z|\tfrac{7}{2}\tfrac{5}{2}\rangle-\langle\tfrac{5}{2}\tfrac{5}{2}|2\hat{S}_z|\tfrac{5}{2}\tfrac{5}{2}\rangle\}=4\langle\tfrac{7}{2}\tfrac{5}{2}\|\Lambda\|\tfrac{5}{2}\tfrac{5}{2}\rangle^2\{5(g_{7/2}-g_{5/2})\}, \quad \text{(A2)}$$

where $g_{5/2}=2/7$, $g_{7/2}=52/63$, and $\langle\frac{7}{2}\frac{5}{2}\|\Lambda\|\frac{5}{2}\frac{5}{2}\rangle^2=15/98$: see Table 2 of Ref. 13.

Similarly, the energy of the final state of the intermultiplet transition $|\frac{7}{2}\frac{7}{2}\rangle$ is only affected by virtual transitions to and from $|\frac{9}{2}\frac{7}{2}\rangle$, which according to Landé's interval rule is situated $\frac{9}{2}\lambda=\frac{9}{7}\Delta_{so}$ higher in energy. Taking into account that $\langle\frac{9}{2}\frac{7}{2}|2\hat{S}_z|\frac{7}{2}\frac{7}{2}\rangle^2=1456/405$, Ref. 13, and $g_{9/2}=106/99$, we get

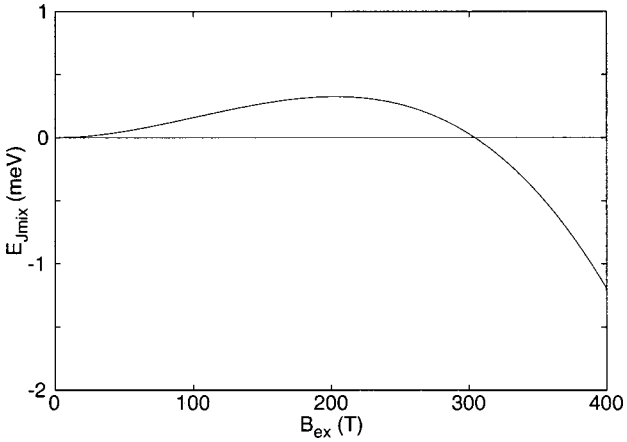

FIG. 2. Correction to E_{inter} due to J mixing as given by Eq. (A4) vs B_{ex}.

$$E_{7/27/2}=-\frac{23}{2}\lambda-\frac{11}{9}\mu_B B_{ex}-\frac{10\,192}{3645}\frac{(\mu_B B_{ex})^2}{\Delta_{so}}+\frac{2\,425\,696}{649\,539}\frac{(\mu_B B_{ex})^3}{\Delta_{so}^2}. \quad \text{(A3)}$$

Subtracting Eq. (A2) from Eq. (A3) and comparing the result with Eq. (4), one arrives at the conclusion that the effect of J mixing consists in incrementing Eq. (4) by the following amount:

$$E_{J\,mix}=0.877\frac{(\mu_B B_{ex})^2}{\Delta_{so}}-6.178\frac{(\mu_B B_{ex})^3}{\Delta_{so}^2}. \quad \text{(A4)}$$

As can be appreciated from Fig. 2, for relevant values of B_{ex} the correction to E_{inter} due to J mixing is negligible in comparison with the experimental error, ± 2 meV.

APPENDIX B: INFLUENCE OF CRYSTAL FIELD ON E_{inter}

The influence of the crystal field on the eigenvalues E_{JM} is described, in the first approximation, by adding to Eq. (3) terms containing diagonal matrix elements of the Stevens operators $\langle JM|O_n^0|JM\rangle$. Irrespective of the symmetry of the crystal, there are just three such terms, for $n=2,4,6$.

We begin with the second-order term. The eigenvalues E_{JM}, as given by Eq. (3), receive the following corrections:

$$\alpha_J[3M^2-J(J+1)]\mathcal{A}_2^0\langle r^2\rangle. \quad \text{(B1)}$$

Here the expression in square brackets is the expectation value of the Stevens operator O_2^0. The prefactor α_J is the Stevens coefficient, regarded herein as a quantity which depends on the quantum number J:

$$\alpha_J=\frac{(2J)^2(2J+2)^2+6(2J)(2J+2)+6885}{180(2J-1)(2J)(2J+2)(2J+3)}. \quad \text{(B2)}$$

This formula is just an adaptation of the general equation due to Judd[39] for the ground LS term of samarium (f^3;^{6}H).

The sought quantity $E_{inter}=E_{7/2,7/2}-E_{5/2,5/2}$ is obtained by adding the corrections (B1) to the right-hand side of Eq. (4), which results in

$$E_{\text{inter}} = \Delta_{\text{so}} + \tfrac{148}{63}\,\mu_B B_{\text{ex}} + (21\alpha_{7/2} - 10\alpha_{5/2})\mathcal{A}_2^0\langle r^2\rangle. \tag{B3}$$

Therefore, Eq. (B2) needs to be used just twice to get $\alpha_{5/2}=13/315$ and $\alpha_{7/2}=26/1575$ (the former is of course the usual ground-multiplet Stevens coefficient, as found, e.g., in Table 20 of Ref. 6). Substituting these values in Eq. (B3) and solving it for $\mu_B B_{\text{ex}}$ yields Eq. (6).

Let us briefly consider the effect of the higher-order crystal field. Following exactly the same pattern as above, we arrive at the conclusion that Eq. (B3) should be incremented by the following amount:

$$\begin{aligned}(420\beta_{7/2} - 60\beta_{5/2})\mathcal{A}_4^0\langle r^4\rangle + 1260\,\gamma_{7/2}\mathcal{A}_6^0\langle r^6\rangle \\ \approx -0.235\mathcal{A}_4^0\langle r^4\rangle + 0.192\mathcal{A}_6^0\langle r^6\rangle.\end{aligned} \tag{B4}$$

Here the integers are the expectation values of O_4^0 and O_6^0 taken directly from Table 17 of Ref. 6 and it has been taken into account that $\gamma_{5/2}=0$. The rest of the Stevens coefficients for this approximate calculation were taken from the convenient four-digit tabulation given in Ref. 40 (Table 3.4 thereof).

The magnitude of $\mathcal{A}_4^0\langle r^4\rangle$ is unlikely to exceed ~3 meV, whereas for $\mathcal{A}_6^0\langle r^6\rangle$ the estimated upper limit is ~1 meV. The corresponding contributions to E_{inter} are ~0.7 and ~0.2 meV, respectively. These can be neglected since E_{inter} is determined experimentally only to ±2 meV.

[1] M. D. Kuz'min, Phys. Rev. B **51**, 8904 (1995).
[2] P. Tils, M. Loewenhaupt, K. H. J. Buschow, and R. S. Eccleston, J. Alloys Compds. **289**, 28 (1999).
[3] G. H. Dieke, *Spectra and Energy Levels of Rare Earth Ions in Crystals* (Interscience, New York, 1968).
[4] R. Osborn, S. W. Lovesey, A. D. Taylor, and E. Balcar, *Handbook on the Physics and Chemistry of Rare Earths*, edited by K. A. Gschneidner, Jr. and L. Eyring (North-Holland, Amsterdam, 1991), Vol. 14, Chap. 91.
[5] M. Rotenberg, R. Bivens, N. Metropolis, and J. K. Wooten, Jr., *The 3-j and 6-j Symbols* (Technology Press, Cambridge, MA, 1959).
[6] A. Abragam and B. Bleaney, *Electron Paramagnetic Resonance of Transition Ions* (Dover, New York, 1986).
[7] P. Tils, Ph.D. thesis, Universität zu Köln, 1997.
[8] O. Moze, R. Caciuffo, G. Amoretti, J. M. D. Coey, H. S. Li, and B. P. Hu (unpublished).
[9] A. Sippel, L. Jahn, M. Loewenhaupt, D. Eckert, P. Kerschl, A. Handstein, K.-H. Müller, M. Wolf, M. D. Kuz'min, L. Steinbeck, M. Richter, A. Teresiak, and R. Bewley, preceding paper, Phys. Rev. B **65**, 064408 (2002).
[10] P. Fabi, Ph.D. thesis, Universität zu Köln, 1993.
[11] O. Moze, R. Caciuffo, H. S. Li, B. P. Hu, J. M. D. Coey, R. Osborn, and A. D. Taylor, Phys. Rev. B **42**, 1940 (1990).
[12] J. H. Van Vleck, *The Theory of Electric and Magnetic Susceptibilities* (Oxford University Press, Oxford, 1932).
[13] R. Elliott and K. Stevens, Proc. R. Soc. London, Ser. A **218**, 553 (1953).
[14] M. Richter, P. M. Oppeneer, H. Eschrig, and B. Johansson, Phys. Rev. B **46**, 13 919 (1992).
[15] M. Richter, L. Steinbeck, U. Nitzsche, P. Oppeneer, and H. Eschrig, J. Alloys Compds. **225**, 469 (1995).
[16] L. Steinbeck, M. Richter, U. Nitzsche, and H. Eschrig, Phys. Rev. B **53**, 7111 (1996).
[17] M. Liebs, K. Hummler, and M. Fähnle, Phys. Rev. B **46**, 11 201 (1992).
[18] M. T. Hutchings, Solid State Phys. **16**, 227 (1964).
[19] J. P. Perdew and A. Zunger, Phys. Rev. B **23**, 5048 (1981).
[20] The SIC-LSDA $4f$ radial wave function was taken from an independent calculation performed with the optimized LCAO method (Refs. 14 and 16), while the $4f$ states were treated within open-core LSDA in the FPLO (Ref. 21) calculation of the crystal potential in the present work. We do not expect this to significantly affect our results since (a) applying SIC to the $4f$ states leaves the crystal potential virtually unaffected and (b) the influence of the slight difference between the crystal potentials obtained with FPLO and with the optimized LCAO methods on the $4f$ radial wave function is small.
[21] K. Koepernik and H. Eschrig, Phys. Rev. B **59**, 1743 (1999).
[22] D. M. Ceperley and B. J. Alder, Phys. Rev. Lett. **45**, 566 (1980).
[23] K. H. J. Buschow, Rep. Prog. Phys. **40**, 1179 (1977).
[24] J. F. Herbst, J. J. Croat, R. W. Lee, and W. B. Yelon, J. Appl. Phys. **53**, 250 (1982).
[25] K. Hummler and M. Fähnle, Phys. Rev. B **53**, 3272 (1996).
[26] P. Novák, Phys. Status Solidi B **198**, 729 (1996).
[27] S. Buck and M. Fähnle, J. Magn. Magn. Mater. **166**, 297 (1997).
[28] M. Liebs, K. Hummler, and M. Fähnle, J. Magn. Magn. Mater. **124**, 239 (1993).
[29] J. Laforest, Ph.D. thesis, Grenoble, 1981.
[30] J. J. M. Franse and R. J. Radwański, in *Handbook of Magnetic Materials*, edited by K. H. J. Buschow (North-Holland, Amsterdam, 1993), Vol. 7, pp. 307–501.
[31] A. V. Deryagin, N. V. Kudrevatykh, and V. N. Moskalev, Fiz. Met. Metalloved. **54**, 473 (1982).
[32] M. D. Kuz'min and J. M. D. Coey, Phys. Rev. B **50**, 12 533 (1994).
[33] J. M. Alameda, J. M. Givord, and Q. Lu, J. Appl. Phys. **52**, 2079 (1981).
[34] B. Matthaei, J. J. M. Franse, S. Sinnema, and R. J. Radwański, J. Phys. (Paris), Colloq. **49**, C8-533 (1988).
[35] S. Brennan, R. Skomski, O. Cugat, and J. M. D. Coey, J. Magn. Magn. Mater. **140–144**, 971 (1995).
[36] J. M. D. Coey, Phys. Scr. **T39**, 21 (1991).
[37] L. Steinbeck, M. Richter, and H. Eschrig, Phys. Rev. B **63**, 184431 (2001).
[38] P. Svoboda, M. Divis, J. Bischof, Z. Smetana, R. Cerny, and J. Burianek, Phys. Status Solidi A **119**, K67 (1990).
[39] B. Judd, Proc. R. Soc. London, Ser. A **251**, 134 (1959).
[40] H.-S. Li and J. M. D. Coey, in *Handbook of Magnetic Materials*, edited by K. H. J. Buschow (North-Holland, Amsterdam, 1991), Vol. 6, pp. 1–83.